Journal of Fluorescence (2019) 29:417–424
https://doi.org/10.1007/s10895-019-02350-y

ORIGINAL ARTICLE

Hydrophilic Truxene Derivative as a Fluorescent off-on Sensor for Copper (II) Ion and Phosphate Species

Pornpat Sam-ang [1,2] · Komthep Silpcharu [1] · Mongkol Sukwattanasinitt [1,3] · Paitoon Rashatasakhon [1,3]

Received: 25 November 2018 / Accepted: 14 January 2019 / Published online: 28 January 2019

Abstract

A new symmetrical truxene derivative (**TP3**) containing three dipicolylamino peripheral groups is successfully synthesized in four synthetic steps with an overall yield of 42%. This hydrophilic fluorescent compound exhibits a maximum absorption wavelength at 375 nm, an emission maximum at 474 nm with an outstanding 58% quantum efficiency in THF-HEPES buffer mixture. The compound shows a highly selective fluorescence quenching towards Cu(II) ion with a detection limit of 0.06 ppm. The results from mass spectrometry and Job plot indicate that a 1:1 complex between **TP3** and Cu(II) ion is responsible for the signal quenching. Interestingly, this **TP3**-Cu complex can be used as a turn-on sensor for hydrogen phosphate and nucleoside phosphates. The limit of detection for hydrogen phosphate is estimated at 8.7 nM. The signal restoration involves a displacement of **TP3** in the complex by the phosphates which have strong coordination abilities with Cu(II) ion.

Keywords Fluorescence · Sensor · Picolylamine · Truxene · Copper (II) ion · Phosphate

Introduction

The design and development of chemosensors for selective detection of ions in aqueous media have long been a significant research subject since many ions play important roles in chemical, biological, and environmental processes [1–5]. For instance, essential metal ions such as Cu(II) plays important roles in a broad range of metabolic pathways, metalloenzymes or biochemical reactions in humans, animals, and plants [6]. However, the over-accumulation of Cu(II) ion can lead to neurodegenerative diseases such as Alzheimer's, Wilson's, and Parkinson's diseases [7–10]. On the other hand, phosphate ions and related organophosphate species are vital components in nucleic acid found in all living organisms. Many of them can be used as herbicides and insecticides in agrochemical applications. In the environment, water-soluble phosphate ions can promote the growth of algae and phytoplankton leading to the reduction of dissolved oxygen level [11–13]. Therefore, the monitoring of phosphate ions in the aquatic environment can be an early notice for declining water quality.

Conventional techniques such as flow-injection analysis, high-performance liquid chromatography, ion chromatography, and electrochemical analysis are routinely used for the detection of ions [14–17]. Those techniques required costly instruments, tedious sample preparations, and skillful operators. In contrast, the fluorescence spectroscopy which requires a relatively inexpensive instrument can provide several advantages such as simple operation, high sensitivity and selectivity, and the ability for on-site or real-time monitoring [18]. A few review articles on selective fluorescent sensors for Cu(II) ion and phosphate have been published [19, 20]. However, the design of Cu(II) sensor using nanoparticulate approach has recently gained much attention [21–26]. On the other hand, recent examples of newly designed phosphate sensors are derivatives of julolidine [27], quinolone [28], 1,8-naphthalene [29], and rhodamine [30]. In this paper, we report the synthesis of a new truxene derivative (**TP3,** Fig. 1) bearing hydrophilic diethyleneglycol units to facilitate its water solubility and three dipicolylaniline groups as metal

Electronic supplementary material The online version of this article (https://doi.org/10.1007/s10895-019-02350-y) contains supplementary material, which is available to authorized users.

✉ Paitoon Rashatasakhon
paitoon.r@chula.ac.th

[1] Department of Chemistry, Faculty of Science, Chulalongkorn University, Bangkok 10330, Thailand

[2] Faculty of Science and Technology, Pibulsongkram Rajabhat University, Phitsanulok 65000, Thailand

[3] Nanotec-CU Center of Excellence on Food and Agriculture, Department of Chemistry, Faculty of Science, Chulalongkorn University, Bangkok 10330, Thailand

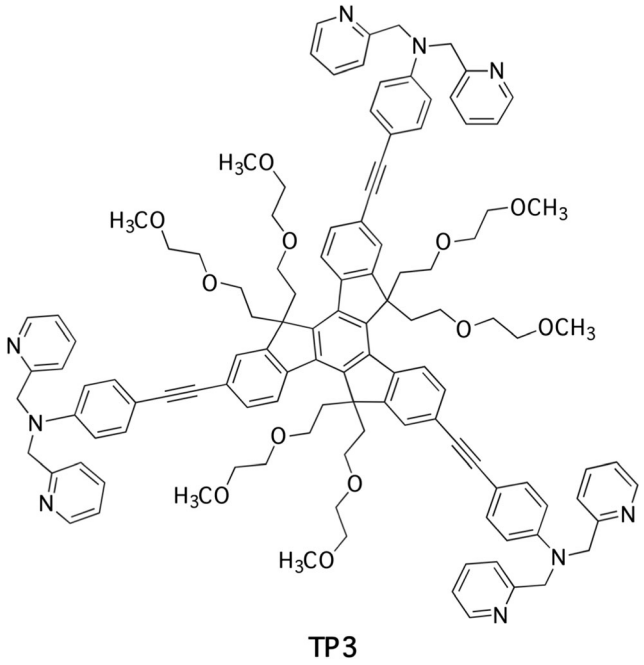

Fig. 1 Structure of **TP3**

ion receptor. This hydrophilic and strongly emissive truxene core has been a subject of interest in our group [31], while the dipicolylamine (DPA) receptor is known as a good chelator for a few metal ions [32–38]. We postulate that the initial binding between **TP3** and a metal ion should result in an alteration of emission signal, and a subsequent competitive binding between that metal ion and an anion should lead to a fluorescence restoration.

Experimental

Materials and Instruments

All reagents and solvents used in the reactions were of standard analytical grade purchased from Fluka (Switzerland), Sigma-Aldrich (USA), or Merck (Germany) and used without further purification. The hydrophilic triiodotruxene core (**3**) was prepared from 3-phenylpropionic acid according to a literature procedure [31]. In anhydrous reactions, solvents such as tetrahydrofuran (THF) and toluene were dried and distilled before use according to standard procedures. Analytical thin layer chromatography (TLC) was performed on silica gel plates (Kieselgel 60, F_{254}, 1 mm). Flash column chromatography was carried out on Merck Kieselgel 60H silica gel and eluting with the solvent system stated in the procedure. ^{1}H NMR spectra were determined on a Varian Mercury NMR spectrometer operating at 400 MHz [13].C NMR spectra were determined on a Bruker Avance NMR spectrometer operating at 100 MHz. Mass spectrum data were obtained by high-resolution electron spray ionization mass spectrometer (HR-ESI-MS) and matrix-assisted laser desorption ionization-time of flight on a Bruker mass spectrometer (MALDI-TOF MS) using α-cyano-4-hydroxycinnamic acid (α-CCA) as a matrix. Absorption spectra were measured by using Shimadzu UV-2550 UV-vis spectrophotometer with a quartz cuvette (path length, 1 cm). Emission spectra were recorded on a Varian Cary Eclipse fluorescence spectrophotometer.

Synthetic Procedures

4-Iodo-2,2′-Dipicolylamine (1) This compound was prepared according to a reported procedure with a slight modification [39]. The mixture solution of 2-(chloromethyl) pyridinium chloride (1.30 g, 8.00 mmol) in water (3 mL) was added with potassium iodide (0.70 g, 4.80 mmol). The potassium carbonate was dissolved in water (3 mL) and slowly added to a mixture solution. Then, a solution of 4-iodoaniline (0.70 g, 4.80 mmol) in acetonitrile (2 mL) was added to the stirred mixture. The reaction mixture was stirred at room temperature for 4 days., and was diluted with water (30 mL). The organic layer was separated and the aqueous phase was extracted with dichloromethane (3 × 20 mL) and was then dried over anhydrous $MgSO_4$. The filtrate was evaporated and the residue was further purified by a silica gel column using gradient solvents starting from 10%EtOAc to CH_2Cl_2 and to EtOAc as an eluent to afford **1** as yellow needle crystals (0.57 g, 44%). IR (KBr) ν_{max} cm^{-1}: 3269, 2099, 1513, 1435, 1344, 1174, 810, 751. ^{1}H-NMR (400 MHz, $CDCl_3$): δ 8.58 (d, J = 4.8 Hz, 2H), 7.62 (t, J = 8.0 Hz, 2H), 7.38 (d, J = 8.0 Hz, 2H), 7.25–7.10 (m, 2H), 6.48 (d, J = 8.0 Hz, 2H), 4.79 (s, 4H) [13].C-NMR (100 MHz, $CDCl_3$): δ 158.2, 149.7, 147.8, 137.8, 136.8, 122.2, 120.7, 114.9, 78.3, 57.3.

4-Ethynyl-2,2′-Dipicolylamine (2) A mixture of **1** (0.30 g, 0.75 mmol), $Pd(PPh_3)_2Cl_2$ (0.03 g, 0.04 mmol) and CuI (0.01 g, 0.04 mmol) in 5 mL of NEt_3-PhMe mixture (1:4 *v*/v) was purged with nitrogen gas for 15 min. Then a portion of trimethylsilylacethylene (0.13 mL, 0.90 mmol) was added to the mixture, and the reaction was stirred overnight under nitrogen atmosphere at room temperature. The solvent was evaporated, and the residue was diluted with dichloromethane (30 mL) and poured into water (20 mL). The organic layer was washed with brine, dried over anhydrous $MgSO_4$, and filtered. The solvent was evaporated and the crude product was purified by column chromatography on neutral alumina

using hexane as a solvent to afford TMS-protected alkyne as a pale yellow solid (0.21 g, 75%). ^{1}H-NMR (400 MHz, $CDCl_3$): δ 8.39 (d, J = 4.8 Hz, 2H), 7.42 (t, J = 7.7 Hz, 2H), 7.06 (d, 8.0 Hz, 2H), 7.01–6.99 (m, 4H), 6.40 (d, J = 8.9 Hz, 2H), 4.62 (s, 4H), 0.00 (s, 9H). ^{13}C-NMR (100 MHz, $CDCl_3$): δ 158.7, 150.1, 148.6, 137.5, 133.8, 122.7, 121.4, 112.7, 111.9, 106.3, 92.1, 57.6, 0.5. To a solution of the TMS-protected alkyne (0.21 g, 0.65 mmol) in THF/MeOH 1:10 *v*/v (5 mL) was added a solution of KOH (2 g) in THF/MeOH 1:10 v/v (5 mL). After the mixture was stirred at room temperature for 30 min, the volatile solvent was removed under reduced pressure, and the residue was dissolved in CH_2Cl_2 (30 mL). The organic solution was washed with NH_4Cl solution, water (20 mL), brine solution (20 mL), and dried over anhydrous $MgSO_4$. The filtrate was evaporated and the residue was eluted through a neutral alumina column by using hexane to provide terminal alkyne **2** as pale yellow crystal (0.17 g, 89%). ^{1}H-NMR (400 MHz, $CDCl_3$): δ 8.57 (d, J = 4.8 Hz, 2H), 7.61 (td, J = 7.7, 1.7 Hz, 2H), 7.29–7.24 (m, 2H), 7.21–7.14 (m, 4H), 6.62 (d, J = 9.0 Hz, 2H), 4.81 (s, 4H), 2.92 (s, 1H). ^{13}C-NMR (100 MHz, $CDCl_3$): δ 158.6, 150.2, 148.8, 137.2, 133.8, 122.5, 121.1, 112.6, 110.5, 84.7, 75.4, 57.6. LR-ESI-MS m/z calcd for $C_{20}H_{17}N_3$: 299.1412, found: 300.07 (M + 1).

TP3 A mixture of triiodotruxene core **3** (0.15 g, 0.11 mmol), $Pd(PPh_3)Cl_2$ (4 mg, 0.05 mmol), CuI (2 mg, 0.05 mmol), and alkyne **2** (0.13 g, 0.45 mmol) was dissolved in toluene (10 mL). Then, 1,8-diazabicyclo[5.4.0] undec-7-ene (DBU, 0.13 mL) was added into the reaction mixture and the stirring was continued at room temperature for 24 h. After the combined filtrate was evaporated and the residue was eluted through a silica gel column by gradient solvents from methylene chloride to ethyl acetate as an eluent to give **TP3** as a yellow solid (0.87 g, 42%). IR (KBr) ν_{max} cm^{-1}: 2921, 2857, 2184, 1590, 1518, 1434, 1347, 1096, 814, 751; ^{1}H-NMR (400 MHz, $CDCl_3$): δ 8.59 (d, J = 4.5 Hz, 2H), 8.21 (d, J = 8.4 Hz, 1H), 7.66–7.62 (m, 3H), 7.45 (dd, J = 15.2 Hz, 7.1 Hz), 7.39 (d, J = 8.4, 2H), 7.26–7.12 (m, 4H), 6.68 (d, J = 8.8 Hz, 2H), 4.86 (s, 4H), 3.20–3.16 (m, 12H), 3.07–2.98 (m, 4H), 2.69–2.64 (m, 4H), 2.54–2.47 (m, 4H); ^{13}C-NMR (100 MHz, $CDCl_3$): δ 158.3, 151.9, 149.8, 148.3, 143.9, 137.9, 137.6, 137.2, 133.2, 130.7, 125.8, 125.1, 123.2, 122.4, 121.1, 112.6, 111.5, 91.6, 88.1, 71.7, 70.0, 67.3, 59.0, 57.3, 51.6, 36.2. MALDI-TOF calcd for $C_{117}H_{123}N_9O_{12}$: 1846.9325, found: 1847.949 (M + 1). HR-ESI-MS m/z calcd for $C_{117}H_{123}N_9O_{12}$: 1846.9325, found: 1847.9404 (M + 1).

Scheme 1 Synthesis of **TP3**

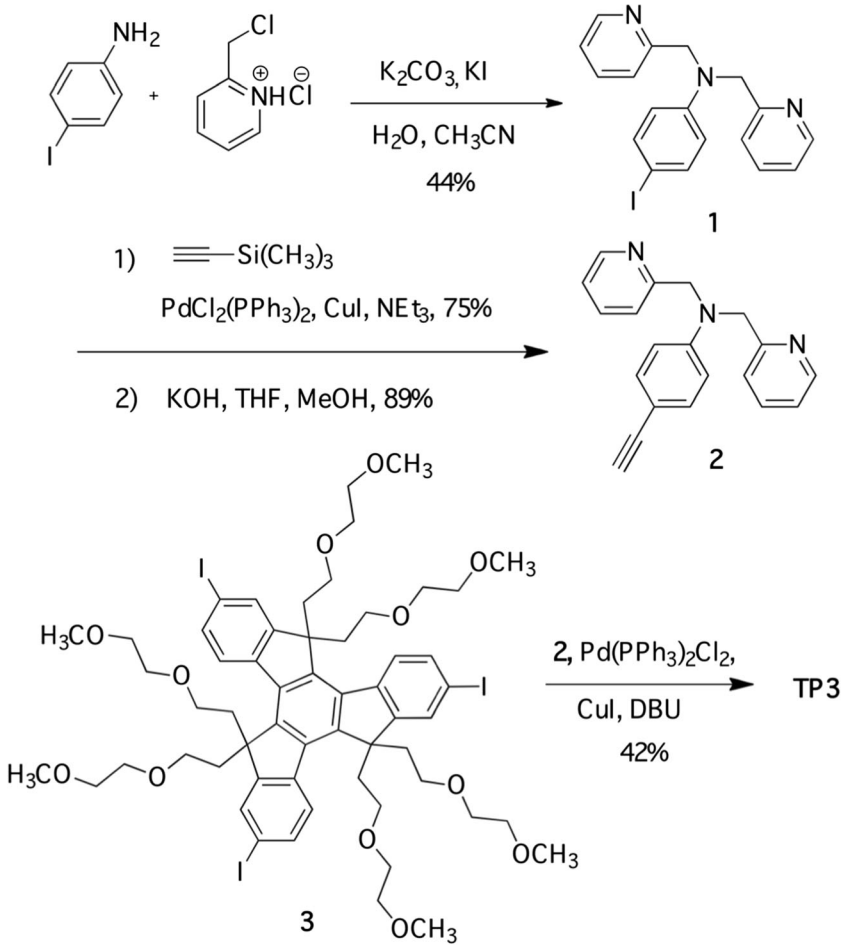

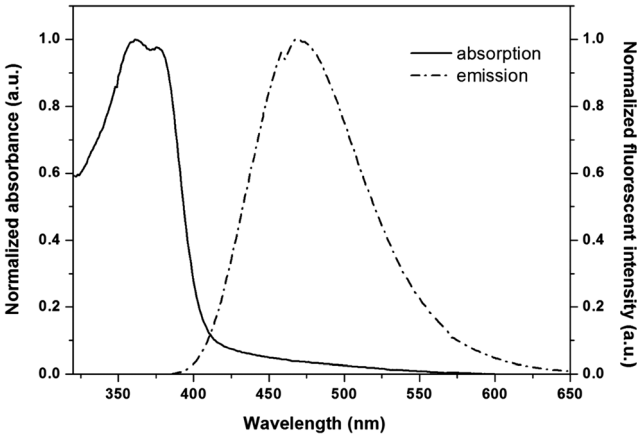

Fig. 2 Normalized absorption and emission spectra of **TP3** in 30% THF-HEPES buffer (2.0 mM, pH 7.4)

Results and Discussion

Synthesis of TP3

The synthesis of **TP3** began with a dialkylation of the commercially available 4-iodoaniline (Scheme 1). Upon treatment with 2-picolyl chloride in a mixture of H_2O and CH_3CN, the *N*,*N*-dipicolyl 4-iodoaniline [39] (**1**) was obtained in 44% yield. It should be noted that the monoalkylated product was also formed as a separable side product in 15%. The Sonogashira cross-coupling between **1** and trimethylsilylacetylene provided the expected product in 75% yield and the subsequent desilylation using KOH in THF and MeOH afforded the alkyne **2** in 89% yield. Meanwhile, the hydrophilic triiodotruxene core **3** was prepared from dihydrocinnamic acid according to our previously reported procedures [31]. The Sonogashira coupling between **3** and terminal alkyne **2** finally provided compound **TP3** in 42% yield. The characterization of **TP3** was performed by several techniques including IR, ^{1}H-NMR, ^{13}C-NMR, MALDI-TOF, and HRMS (Fig. S1-S3).

Photophysical Properties

After a successful synthesis and characterization of **TP3**, its stock solution in THF at 1.0 mM was prepared and diluted to the desired concentration with HEPES buffer (2.0 mM, pH 7.4). Since we planned to used **TP3** as a turn-off sensor, we then first screened for a mixed solvent system that could provide the highest emission signal of **TP3**. Data in Fig. S4 showed that emission of **TP3** drastically dropped when the aqueous buffer content increased from 70 to 80%, presumable due to low water-solubility of **TP3**. Therefore, a 70:30 mixture between HEPES buffer and THF was used as the medium for this study. The normalized absorption and emission spectra of **TP3** in this selected solvent system are shown in Fig. 2 while the excitation spectrum is shown in Fig. S5. There is a characteristic absorption band of phenylacetylene-conjugated truxene at 375 nm with a molar extinction coefficient of 4.85 M^{-1} cm^{-1}. Upon an excitation at the absorption maxima, **TP3** showed an emission peak at 474 nm. In comparison to the parent truxene which has a 6% quantum yield in aqueous THF [40], **TP3** exhibit an outstanding quantum yield of 58%. This compound has a large stoke shift of 99 nm, probably due to a substantial non-radiative energy loss of the excited fluorophore by the rotation of the three dipicolyl peripheries.

Selectivity Screening

The selectivity of **TP3** at 5 μM in 30% THF-HEPES buffer (2.0 mM, pH 7.4) were tested with a number of metal ions at 50 μM. It was found that the fluorescent signal of **TP3** was selectively quenched by Cu(II) (Fig. 3). On the absorption

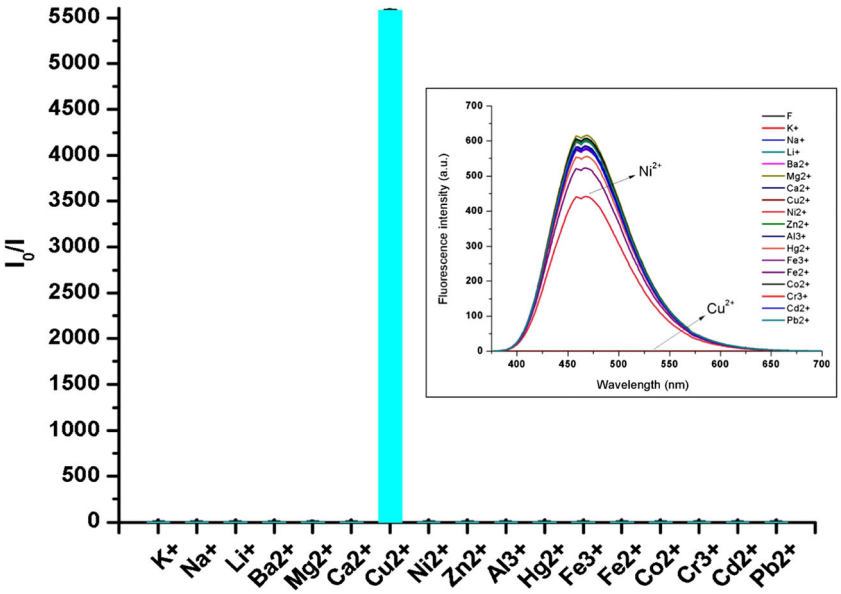

Fig. 3 Fluorogenic responses of **TP3** (5 μM) towards various metal ions (50 μM) in 30% THF-HEPES buffer (2.0 mM, pH 7.4)

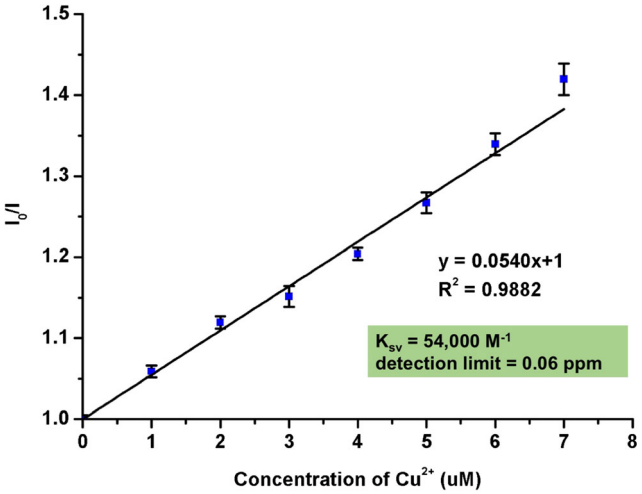

Fig. 4 Stern-Volmer plot of the fluorescence quenching of **TP3** by Cu^{2+}

spectra (Fig. S6), the addition of copper(II) ion caused a spectral shift from 375 nm to 336 nm. These spectral changes possibly resulted from a selective and strong coordination between Cu(II) and the dipicolylamine moiety. From a fluorescence titration of **TP3** by Cu(II) (Fig. S7), a linear Stern-Volmer plot with an equation $I_0/I = 5.4 \times 10^4$ [Q] + 1 was obtained (Fig. 4), where I_0 and I represented the fluorescence intensities before and after the addition of quencher, [Q] was the concentration of Cu(II), and the Stern-Volmer constant of 5.4×10^4 was estimated from the slope. The limit of detection (LOD = 3σ/K) of Cu(II) at three-time-noise was determined as 0.06 ppm.

Cu(II) Sensing Mechanism

Since the addition of EDTA into a mixture of **TP3** and Cu(II) could fully recover the fluorescent signal (Fig. 5a), it is likely that a complex formation is responsible for signal quenching. A Job plot in Fig. 5b was established in order to determine the binding stoichiometry between **TP3** with Cu(II). The result suggested that the maximum quenching efficiency was observed at 0.5 mol fraction of Cu(II), indicating a 1:1 stoichiometry between **TP3** and Cu(II). Since **TP3** contains three binding sites, it might be possible that the initial binding to the first Cu(II) ion is the most significant cause of the fluorescent quenching. This 1:1 complex may be non-fluorescent due to the paramagnetic nature of Cu(II) [41], thus additional binding to the second and third Cu(II) ions may not cause further fluorescent change. In fact, when a mixture of **TP3** (10 μM) and Cu(II) (100 μM) in 30% THF-HEPES buffer (2.0 mM, pH 7.4) was subjected to MALDI-TOF analysis, a molecular ion with m/z of 1910.704 was detected (Fig. S8). This signal corresponded to the exact mass of a stable **TP3** complex with Cu(I) ion, which could derive from the reduction of Cu(II) by HEPES buffer [42]. The complex formation constant between **TP3** and Cu(II) was estimated to 1.72×10^5 using Benesi-Hildebrand plot shown in Fig. S9 [43].

Anion Sensing by TP3-Cu Complex

The selective fluorescent quenching of **TP3** by Cu(II) led us to further investigate the use of this complex as an anion sensor. For the selectivity screening, a number of common anions such as HPO_4^{2-}, ClO_4^-, SO_4^{2-}, NO_3^-, OAc^-, SO_3^{2-}, CN^-, CO_3^{2-}, F^-, Cl^-, Br^- and I^-, and a few nucleoside phosphates such as ATP, ADP and AMP were added to solutions containing **TP3** (10 μM) and Cu(II) (100 μM) in 30% THF-HEPES buffer (2.0 mM, pH 7.4). Interestingly, data from fluorescent spectra (Fig. 6) showed that the signal of **TP3** could be restored by HPO_4^{2-} and the three nucleoside phosphates. The UV-vis absorption spectra in Fig. S10 suggested a release of

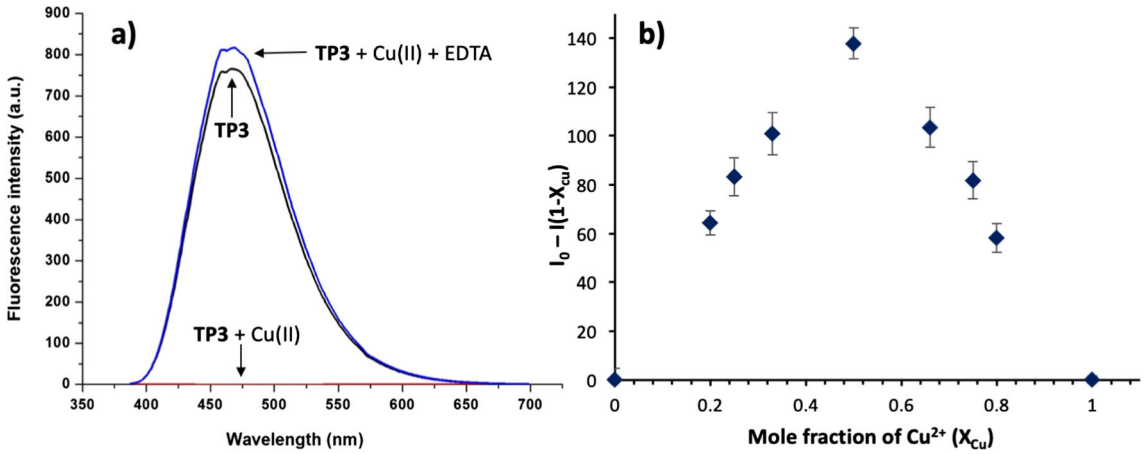

Fig. 5 **a**) Fluorescence signals of **TP3** (10 μM) in the presence of Cu(II) (100 μM) and EDTA (100 μM) in 30% THF-HEPES buffer (2.0 mM, pH 7.4), **b**) Job plot of the complexation between **TP3** and Cu(II)

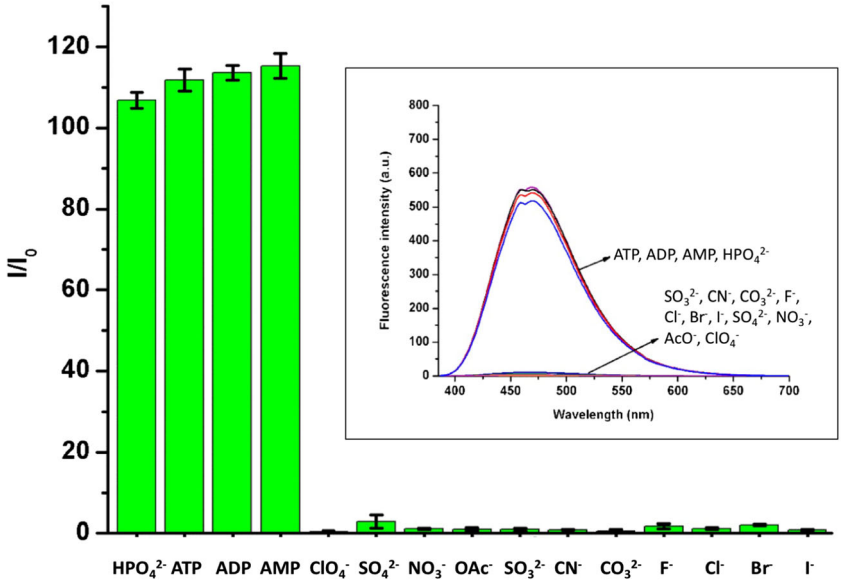

Fig. 6 Fluorescent enhancement ratio (I/I_0) of complex (**TP3**-Cu(II)) (10 μM) after addition of each analyte (100 μM, 10 eq.) in 30% THF-HEPES buffer (2.0 mM, pH 7.4). Inset: emission spectra after addition of each analyte

free **TP3** upon addition of those phosphate species. Therefore, it is likely that the strong binding between HPO_4^{2-} and the nucleoside phosphates with Cu(II) could facilitate the release **TP3** from its complex.

pH Effect on Phosphate Sensing

Due to the amphoteric properties of HPO_4^{2-}, we decided to investigate the pH effect on the sensitivity of **TP3**-Cu(II) complex towards HPO_4^{2-}. For this study, HEPES buffers at pH 6.6, 7.4 and 8.8 were prepared and used as sensing media along with THF. The data in Fig. 7 reveals that the fluorescent intensity of **TP3** was slightly lower under the acidic pH due to partial protonation of the dipicolyl groups. Upon the addition of Cu(II), the intensity was lowered tremendously at pH 6.6 and 7.4, while only 2/3 of the signal was quenched at pH 8.8 which may result from a significant formation of $Cu(OH)_2$ (Ksp 2.2×10^{-20}). When anions were added to **TP3**-Cu(II) mixture, it was observed that only the HPO_4^{2-} could selectively enhance the fluorescent intensity under these three pHs. However, the maximum sensitivity for HPO_4^{2-} sensing ($I_{\mathbf{TP3}+Cu+HPO4}/I_{\mathbf{TP3}+Cu}$) could be observed at pH 7.4. Under the optimal conditions, a linear plot between fluorescence enhancement ratio and concentration of HPO_4^{2-} was constructed (Fig. S11-S12) and a detection limit of 8.7 nM could be estimated.

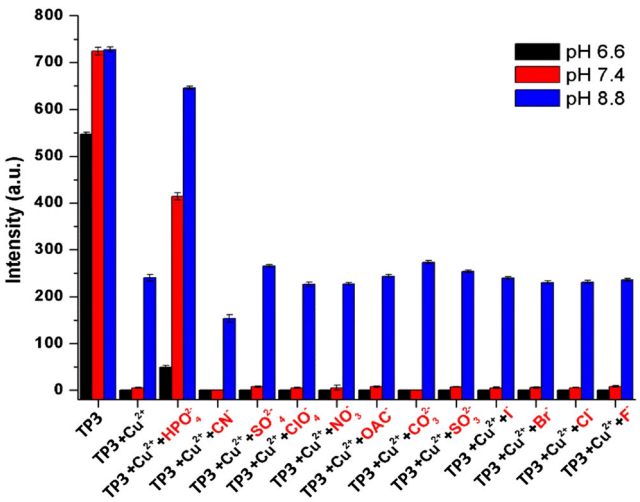

Fig. 7 The fluorescent intensity of **TP3** (5 μM) before and after the addition of Cu(II) (50 μM) and various anions (50 μM) in 30% THF-HEPES buffer at various pH

Conclusion

As a metal ion sensor used in aqueous media, sensor **TP3** comprises hydrophilic diglycol units on the truxene core and dipicolyl amine as binding sites for cation. The greater synthetic efficiency was witnessed as **TP3** was produced in the overall yield of 42% after 4 steps. **TP3** exhibits the absorption maxima at 375 nm and the emission maxima at 474 nm with an outstanding quantum efficiency of 58%. The sensor showed a selective fluorescent response to Cu(II) by exhibiting a blue-shift of absorption band from 375 to 336 nm and a quenching of emission signal. The fluorescent quenching possibly resulted from a selective and stronger coordination between Cu(II) and the dipicolylamine moiety. The Stern-Volmer constant (K_{sv}) was calculated to be 5.4×10^4 M^{-1} with the detection limit of 0.06 ppm. Interestingly, the **TP3-Cu(II)** exhibited selective fluorescent enhancement by HPO_4^{2-} and some biological phosphates such as ATP, ADP, and AMP. The detection limit for HPO_4^{2-} was estimated at 8.7 nM. The fluorescence restoration was presumably due to a competitive binding that removes Cu(II) from its complex with **TP3**.

Acknowledgments This work was supported by the Grant for International Research Integration: Chula Research Scholar and the National Nanotechnology Center (NANOTEC), NSTDA, Ministry of Science and Technology, Thailand, through its program of Research Network NANOTEC (RNN). PS thanks to the Overseas Research Experience Scholarship for Graduate Student, the 90th Anniversary of Chulalongkorn University Fund (Ratchadapiseksomphot fund) and the financial support from the Pibulsongkram Rajabhat University.

References

1. Kaur B, Kaur N, Kumar S (2018) Colorimetric metal ion sensors – A comprehensive review of the years 2011–2016. Coord Chem Rev 358:13–69
2. Gale PA, Caltagirone C (2018) Fluorescent and colorimetric sensors for anionic species. Coord Chem Rev 354:2–27
3. Wong JK-H, Todd MH, Rutledge PJ (2017) Recent Advances in Macrocyclic Fluorescent Probes for Ion Sensing. Molecules 22:200
4. Carter KP, Young AM, Palmer AE (2014) Fluorescent Sensors for Measuring Metal Ions in Living Systems. Chem Rev 114:4564–4601
5. Formica M, Fusi V, Giorgi L, Micheloni M (2012) New fluorescent chemosensors for metal ions in solution. Coord Chem Rev 256: 170–192
6. Scheiber I, Dringen R, Mercer JFB (2013) Copper: Effects of Deficiency and Overload. Met Ions Life Sci 13:359
7. Waggoner DJ, Bartnikas TB, Gitlin JD (1999) The Role of Copper in Neurodegenerative Disease. Neurobiol Dis 6:221–230
8. Strausak D, Mercer JFB, Dieter HH, Stremmel W, Multhaup G (2001) Copper in disorders with neurological symptoms: Alzheimer's, Menkes, and Wilson diseases. Brain Res Bull 55: 175–185
9. Kumar N, Low PA (2004) J Neurol 251:747
10. Halfdanarson TR, Kumar N, Li C-Y, Phyliky RL, Hogan WJ (2008) Hematological manifestations of copper deficiency: a retrospective review. Eur J Haematol 80:523–531
11. Knutsson J, Rauch S, Morrison GM (2013) Environ Sci-Proc Imp 15:955
12. Warwick C, Guerreiro A, Soares A (2013) Sensing and analysis of soluble phosphates in environmental samples: A review. Biosens Bioelectron 41:1–11
13. Berchmans S, Issa TB, Singh P (2012) Determination of inorganic phosphate by electroanalytical methods: A review. Anal Chim Acta 729:7–20
14. Jia X, Chen D, Bin L, Lu H, Zhang R, Zheng Y (2016) Highly selective and sensitive phosphate anion sensors based on AlGaN/GaN high electron mobility transistors functionalized by ion imprinted polymer. Sci Rep 6:27728
15. De Marco R, Pejcic B, Chen Z (1998) Flow injection potentiometric determination of phosphate in waste waters and fertilisers using a cobalt wire ion-selective electrode. Analyst 123:1635–1640
16. Brando C, Hoffman T, Bonvini E (1990) High-performance liquid chromatographic separation of inositol phosphate isomers employing a reversed-phase column and a micellar mobile phase. J Chromatogr B Biomed Sci Appl 529:65–80
17. Sekiguchi Y, Mitsuhashi N, Kokaji T, Miyakoda H, Mimura T (2005) Development of a comprehensive analytical method for phosphate metabolites in plants by ion chromatography coupled with tandem mass spectrometry. J Chromatogr A 1085:131–136
18. Lakowicz JR (2006) Principles of fluorescence spectroscopy. Springer, New York
19. Saleem M, Rafiq M, Hanif M, Shaheen MA, Seo SY (2018) A Brief Review on Fluorescent Copper Sensor Based on Conjugated Organic Dyes. J Fluoresc 28:97–165
20. Lee S, Yuen KKY, Jolliffe KA, Yoon J (2015) Fluorescent and colorimetric chemosensors for pyrophosphate. Chem Soc Rev 44: 1749–1762
21. Fatino A, Steinkruger JD, Hao J, Yang S, Zhou C (2018) Luminescent gold nanoparticles as dual-modality sensors for selective copper (II) ion detection. Mater Lett 232:70–73
22. Qin J, Dong B, Gao R, Su G, Han J, Li X, Liu W, Wang W, Cao L (2017) Water-soluble silica-coated ZnS : Mn nanoparticles as fluorescent sensors for the detection of ultratrace copper(ii) ions in seawater. Anal Methods 9:322–328
23. Shenashen MA, El-Safty SA, Elshehy EA (2013) Architecture of optical sensor for recognition of multiple toxic metal ions from water. J Hazard Mater 260:833–843
24. Viswanathan K (2012) Utilizing a tripeptide conjugated fluorescent hybrid nanoparticles as a fluorescence sensor for the determination of copper ions. Sens Actuator A Phys 175:15–18
25. Zhang J, Li B, Zhang L, Jiang H (2012) An optical sensor for Cu(ii) detection with upconverting luminescent nanoparticles as an excitation source. Chem Commun 48:4860
26. Kirubaharan CJ, Kalpana D, Lee YS, Kim AR, Yoo DJ, Nahm KS, Kumar GG (2012) Biomediated Silver Nanoparticles for the Highly Selective Copper(II) Ion Sensor Applications. Ind Eng Chem Res 51:7441–7446
27. Jang HJ, Ahn HM, Kim MS, Kim C (2017) A highly selective colorimetric chemosensor for sequential detection of Fe 3+ and pyrophosphate in aqueous solution. Tetrahedron 73:6624–6631
28. Liu X, Wang P, Fu J, Yao K, Xue K, Xu K (2017) Turn-on fluorescent sensor for Zinc and Cadmium ions based on quinolone and its sequential response to phosphate. J Lumin 186:16–22
29. Jiang S-Q, Zhou Z-Y, Zhuo S-P, Shan G-G, Xing L-B, Wang H-N, Su Z-M (2015) Rational design of a highly sensitive and selective "turn-on" fluorescent sensor for PO43−detection. Dalton Trans 44: 20830–20833
30. Wang K-P, Zhang S-J, Lv C-D, Shang H-S, Jin Z-H, Chen S, Zhang Q, Zhang Y-B, Hu Z-Q (2017) A highly sensitive and selective turn-on fluorescent sensor for dihydrogen phosphate in living cells. Sens Actuator B Chem. 247:791–796
31. Earmrattana N, Sukwattanasinitt M, Rashatasakhon P (2012) Water-soluble anionic fluorophores from truxene. Dyes Pigments 93:1428–1433
32. Azuma Y, Imai H, Yoshimura T, Kawabata T, Imanishi M, Futaki S (2012) Dipicolylamine as a unique structural switching element for helical peptides. Org Biomol Chem 10:6062–6068
33. Zhang JF, Kim S, Han JH, Lee S-J, Pradhan T, Cao QY, Lee SJ, Kang C, Kim JS (2011) Pyrophosphate-Selective Fluorescent Chemosensor Based on 1,8-Naphthalimide–DPA–Zn(II) Complex and Its Application for Cell Imaging. Org Lett 13:5294–5297
34. O'Neil EJ, Smith BD (2006) Anion recognition using dimetallic coordination complexes. Coord Chem Rev 250:3068–3080
35. Luo H-Y, Zhang X-B, He C-L, Shen G-L, Yu R-Q (2008) Synthesis of dipicolylamino substituted quinazoline as chemosensor for cobalt(II) recognition based on excited-state intramolecular proton transfer. Spectrochim Acta A 70:337–342
36. Hatai J, Bandyopadhyay S (2014) Altered selectivity of a dipicolylamine based metal ion receptor. Chem Commun 50:64–66
37. Xue L, Wang H-H, Wang X-J, Jiang H (2008) Modulating Affinities of Di-2-picolylamine (DPA)-Substituted Quinoline Sensors for Zinc Ions by Varying Pendant Ligands. Inorg Chem 47:4310–4318

38. Chen W-H, Xing Y, Pang Y (2011) A Highly Selective Pyrophosphate Sensor Based on ESIPT Turn-On in Water. Org Lett 13:1362–1365
39. Jiang Z, Deng R, Tang L, Lu P (2008) A new fluorescent chemosensor detecting Zn2+ and Cu2+ in methanol/HEPES buffer solution. Sens Actuator B Chem 135:128–132
40. Sam-ang P, Raksasorn D, Sukwattanasinitt M, Rashatasakhon P (2014) A nitroaromatic fluorescence sensor from a novel tripyrenyl truxene. RSC Adv 4:58077–58082
41. Yang W, Chen X, Su H, Fang W, Zhang Y (2015) The fluorescence regulation mechanism of the paramagnetic metal in a biological HNO sensor. Chem Commun 51:9616–9619
42. Hegetschweiler K, Saltman P (1986) Interaction of copper(II) with N-(2-hydroxyethyl)piperazine-N'-ethanesulfonic acid (HEPES). Inorg Chem 25:107–109
43. Borase PN, Thale PB, Shankarling GS (2016) Dihydroquinazolinone based "turn-off" fluorescence sensor for detection of Cu 2+ ions. Dyes Pigments 134:276–284